Available online at www.sciencedirect.com
ScienceDirect
Trans. Nonferrous Met. Soc. China 23(2013) 699−710
Transactions of Nonferrous Metals Society of China
www.tnmsc.cn

Effect of fluoride treatment on corrosion behavior of Mg−Ca binary alloy for implant application

Hamid Reza Bakhsheshi-Rad[1], Mohd Hasbullah Idris[1], Mohammed Rafiq Abdul Kadir[2], Mohammadreza Daroonparvar[1]

1. Materials Engineering Department, Faculty of Mechanical Engineering, Universiti Teknologi Malaysia, Skudai 81310, Johor, Malaysia;
2. Department of Biomechanics & Biomedical Materials, Faculty of Biomedical Engineering & Health Sciences, Universiti Teknologi Malaysia, Skudai 81310, Johor, Malaysia

Received 24 February 2012; accepted 5 June 2012

Abstract: The influence of hydrofluoric acid (HF) treatment on the corrosion behavior of the Mg−0.5Ca alloys was investigated by immersion specimen in sodium hydroxide and HF solutions with various concentrations and durations at room temperature. Microstructural evolutions of the specimens were characterized by atomic force microscopy, X-ray diffraction, field-emission scanning electron microscopy. The corrosion resistance was examined through potentiodynamic polarization and immersion test in Kokubo solution. The results revealed that the fluoride treated Mg−0.5Ca alloys produced by immersion in 40% HF provided more uniform, dense and thicker coating layer (12.6 μm) compared with the 35% HF treated specimen. The electrochemical test showed that the corrosion resistance of fluoride treated specimen was 35 times higher compared with the untreated Mg−0.5Ca alloy specimen in Kokubo solution. In vitro degradation rate of the fluoride treated specimens was much lower than untreated Mg−0.5Ca alloy in Kokubo solution. After immersion test the surface of 40% HF treated sample showed a few corrosion dots, while untreated specimens were fully covered by corrosion products and delamination. Fluoride treated Mg−0.5Ca alloy with 40% HF is a promising candidate as biodegradable implants due to its low degradation kinetics and good biocompatibility.
Key words: Mg−Ca alloy; surface treatment; corrosion behavior; biocompatibility

1 Introduction

Magnesium and its alloys have now received noticeable attention as candidate materials for temporary medical implants due to its degradable, resorbable and osteoconductive behavior [1,2]. Compared with other biocompatible metals, magnesium has an elastic modulus, compressive yield strength and density near to the natural bone [3−5]. For orthopedic applications in particular, calcium has been identified as one of the alloying elements for magnesium alloys. This is mainly due to the fact that calcium is the main element in human bone and thus improves bone healing through the release of magnesium and calcium ions [6]. The addition of Ca also has the added advantage of increasing the low ignition temperature of the molten Mg alloys by the formation of stable oxide film [7]. Calcium has a low density at a reasonable cost which makes it very attractive to be used commercially as orthopedic implants [8]. The application of magnesium is however hindered due to its relatively poor corrosion resistance, the release of hydrogen gas and high degradation rate when exposed to human body fluid [9−11]. Several reports have shown that decreasing the corrosion rate of Mg in simulated body fluids is possible by surface treatment methods. The surface treatment methods include conversion coatings [12], carbonate treatment [13], hydride coatings [14], alkali-heat-treatment [15] , anodizing [16], polymeric coatings [17] and electrodeposition [18]. Among these methods conversion treatment via hydrofluoric acid is a promising method owing to its simplicity and low cost of the process. By this method, corrosion rate decreases by providing a magnesium fluoride (MgF_2) protective layer on the surface of the substrate. The coating layer (MgF_2) has also been reported to provide high density which is chemically inert and non-toxic as well as reduces water

Corresponding author: Hamid Reza Bakhsheshi-Rad; Tel: +60-147382258; Fax: +60-75534610; E-mail: Rezabakhsheshi@gmail.com; Bhamidreza2@live.utm.my
DOI: 10.1016/S1003-6326(13)62519-4

solubility [19]. Moreover one of the components of human bone and teeth is fluorine [20].

There are numerous literatures on the corrosion behavior of magnesium alloys. CHEN et al [21] and GU et al [22] revealed that micro arc oxidation can decrease the corrosion rates of Mg−Ca alloys by 90%. CHIU et al [3] reported that the fluoride treatment of Mg increased the corrosion resistance in Hanks' solution. ELSENTRIECY et al [23] exhibited that the coating film density and corrosion resistance of AZ91D magnesium alloy improved remarkably by pickling pretreatment. GU et al [15] showed that corrosion rates of Mg−Ca alloys were significantly reduced by alkaline heat treatments. THOMANN et al [20] revealed that Mg−0.8Ca fluoride coated implants possessed good clinical tolerance and good biocompatibility. DRYNDA et al [24] indicated that fluoride-coated magnesium−calcium alloys are suitable candidate materials for cardiovascular stents due to their good degradation kinetics and adequate mechanical properties. However, no studies have been reported on the effect of HF treatment with various concentrations on the corrosion behavior and degradation mechanism of Mg−Ca alloys. Therefore, the main objective of the present study is to investigate the effect of HF treatment with various concentrations and durations of Mg−0.5Ca alloys on degradation behavior and corrosion rate. The untreated and fluoride-coated specimens were characterized by X-ray diffraction, field-emission scanning electron microscopy and energy dispersive X-ray spectroscopy. In addition the electrochemical behaviors of untreated and fluoride-coated specimens were assessed by potentio-dynamic polarization and immersion tests in Kokubo solution.

2 Experimental

2.1 Fabrication and materials preparation

Pure magnesium ingot (99.99% Mg) and calcium−magnesium master alloy (Mg−32Ca) were used as starting materials. The materials were melted under argon gas in a mild steel crucible at 760 °C with a resistance furnace. The molten metal was poured into a preheated mild steel mould. The chemical compositions of the as-cast Mg−0.5Ca alloys are listed in Table 1. Numerous specimens in round (10 mm×5 mm) and cubic (15 mm×8 mm×5 mm) shapes were cut from the ingot and mechanically wet ground with 320 to 4000 SiC grit paper until all visible scratches were removed for microstructural analysis via optical and scanning electron microscopy.

Table 1 Nominal and analyzed compositions of Mg−0.5Ca alloys

Composition	w(Mg)/%	w(Ca)/%
Nominal composition	99.5	0.5
Analyzed composition	99.47	0.53

2.2 HF treatment and characterization

For surface treatment the polished specimens were washed entirely with distilled water, rinsed and ultrasonically degreased with ethanol and dried in a warm stream of air. Then the specimens were immersed in 250 g/L sodium hydroxide solution (NaOH) for duration of 2 h. Subsequently, they were cleaned in distilled water and dried in air. From that time on, the specimens were immersed in different concentrations of hydrofluoric acid (5%, 10%, 20%, 35%, 40% and 48% HF) and durations for 6, 12, 18 and 24 h at room temperature. The treatment specimens were washed with deionized water, dried and subsequently assessed visually for the uniformity of coating layer. To evaluate the mass change, the specimens before and after the immersion was measured by using analytic balance. The morphology of untreated and fluoride coated samples were analyzed using scanning electron microscopy (SEM, Jeol Jsm-6380LA) equipped with energy dispersive spectroscopy (EDS, Zeiss Supra 33VP). The thickness of the fluoride coated specimens was measured by field-emission scanning-electron microscopy (FESEM, Jeol Jsm−6390). X-ray diffractometry (XRD, Siemens-D500) was used to evaluate phases present in the untreated and treated specimens using Cu K_α line generated at 40 kV and 35 mA. The surface topography of the treated and untreated specimens was evaluated by using atomic-force microscopy (AFM, NanoScope IV, Digital Instruments) in the tapping mode.

2.3 Electrochemical tests

Electrochemical tests were conducted using potentiodynamic polarization in Kokubo solution with pH 7.66 at a temperature of 37 °C and open to air. Three-electrode cell was used for electrochemical measurements: the counter electrode was made of graphite rod, the working electrode was the specimen and the reference electrode was saturated calomel electrode (SCE). For the fluoride coated and untreated specimens potential scanning rate was carried out at a constant scan rate of 0.5 mV/s initiated at −250 mV below the open circuit potential. An area of 1 cm^2 on the specimen was exposed to the solution. Three to four measurements were carried out for each treatment condition as well as for the untreated samples.

2.4 Immersion test

The immersion tests of fluoride coated and untreated specimens were conducted according to ASTM

G31—72 standard [25]. The specimens were immersed in 150 mL beaker of Kokubo simulated body fluid (SBF) at pH 7.66 for in vitro test. The beakers were sealed and then incubated at constant temperature of (37±1) °C for 7 d. Afterwards, the specimens were rinsed with acetone, deionized water and corrosion products were removed before mass measurement. The corrosion rate was calculated as follows:

$$R_c=m/(Atd) \quad (1)$$

where R_c is the corrosion rate, m is the mass loss, A is the surface area exposed to the corrosive media, t is the exposure time, and d is the density [25]. The average pH of the SBF from three measurements was recorded during the soaking experiment after 12 h intervals. After immersion test, the surface appearance of corroded specimens was assessed by using SEM and EDS.

3 Results and discussion

3.1 Preparation of specimens

Mg alloys soaked in NaOH solution reacted with sodium hydroxide and formed a thick $Mg(OH)_2$ layer and then by soaking sample into the hydrofluoric acid the $Mg(OH)_2$ transformed into insoluble barrier layer of MgF_2 according to Eqs. 2 and 3 [3,17].

$$Mg+2NaOH=Mg(OH)_2+2Na \quad (2)$$

$$Mg(OH)_2+2HF\longrightarrow MgF_2+2H_2O \quad (3)$$

Figure 1 exhibits the effect of hydrofluoric acid treatment time at various concentrations on the mass change of specimens. It can be seen that when the treatment time increased to 12 h, the mass gained considerably to 2.5 and 2.1 mg/cm^2 corresponding to 35% and 40% HF respectively, indicating a high growth rate of protective layer (MgF_2) formation. As a comparison with the curve slope mass gain in 5% and 10% HF is lower than other HF concentration due to lower protective layer formation rate. The enhancement of mass gain with increasing deposition of MgF_2 layer was due to the reaction between magnesium alloy and hydrofluoric acid. CONCEICAO et al [17] reported that the slow kinetics reaction of Mg alloy with HF was related to the barrier nature of MgF_2. Beyond 12 h of treatment time the mass gained gradually for 10%, 35% and 40% HF as a result of moderate growth rate of MgF_2 layer formation. The slope of the mass curve decreased with increasing immersion time from 18 to 24 h for all specimens as a consequence of decline in deposition rate. These results were in agreement with previous published reports [3] which suggested that the growth of deposit can be developed at the film/metal interface due to high mobility of F ions. Hence, growth of deposit decreases with increasing film thickness. It is also evident that for specimen treated with 35% and 40% HF the protective layer formation has inclination to reach the yield and saturation. Similar behavior is predicted for other treated specimens in immersion time higher than that for 24 h. Figure 2 shows that by increasing HF concentration from 5% to 40% the film thickness increased while the film thickness of 48% HF treated specimen decreased. It can be attributed to a higher dissolution rate of specimens at concentration of 48% HF. By comparison the result of immersion time versus HF concentration and mass gain as well as HF concentration versus film thickness, the 35% and 40% HF treated specimens with immersion time of 24 h were selected for further investigation.

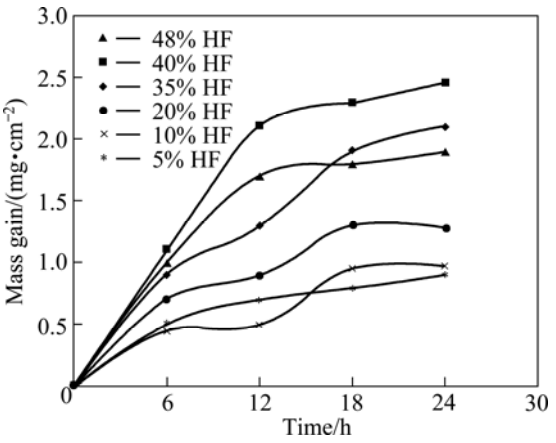

Fig. 1 Variation of mass gain of treated specimens in HF solution as function of immersion time

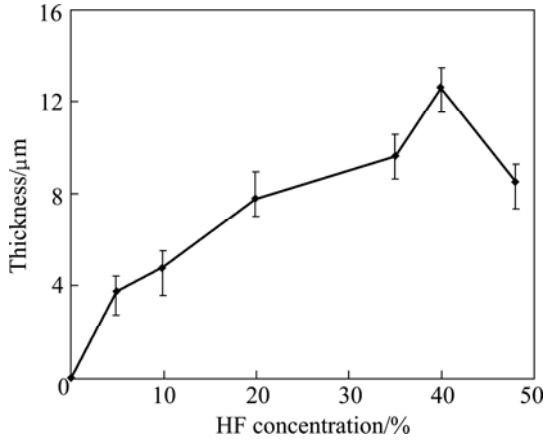

Fig. 2 Variation of coating thickness vs HF concentration in constant immersion time of 24 h

Figure 3 shows top view of specimens soaked in 35% HF and 40% HF solutions for 24 h immersion duration. After passivation in hydrofluoric acid, the deposition of compounds on the surface of specimen is clearly distinctive. It was clearly seen that the entire specimen surface was covered via a passive film. These results confirmed the attainment of mass gain for samples treated with 35% HF and 40% HF. However, the

specimens treated with 35% HF had irregular morphology compared with 40% HF, and possessed an almost uniform golden color with some light brown area. On the other hand, the specimens treated with 40% HF had black color with some dark bluish area. The difference between the appearances of specimens could be the result of different compounds present on the surface of specimen.

3.2 Microstructure and coating characterization

Figure 4 shows SEM images of untreated and fluoride treated samples after being soaked for 24 h in hydrofluoric acid. Figure 4(a) indicates that the microstructure of untreated Mg−0.5Ca alloys consists of α-Mg matrix and Mg_2Ca intermetallic phase. It can be seen that the Mg_2Ca phase located on the grain boundaries, triple conjunction of grain boundary and within grains of α-Mg matrix. The SEM images of a treated sample (Figs. 4(b) and (c)) depict that the surface of specimen was completely covered with a thin layer with irregular morphology. The SEM image of the cross-sections of 35% HF and 40% HF treated specimens and the corresponding EDS after 24 h are shown in Fig. 5. From Fig. 5, it can be observed that the dense and uniform passive films with average thickness around 9.2 μm and 12.6 μm were deposited on 35% HF and 40% HF treated specimens, respectively. DRYNDA et al [24] reported that the deposition of MgF_2 layer of 15−20 μm delayed the initiation of the corrosion processes. The EDS analysis of 35% HF and 40% HF treated

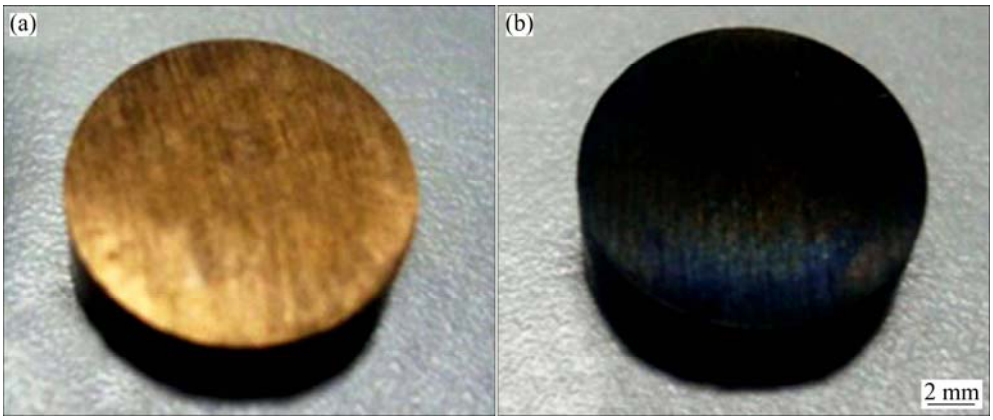

Fig. 3 Photos of 35% HF (a) and 40% HF (b) treated specimens after fluoride treatment

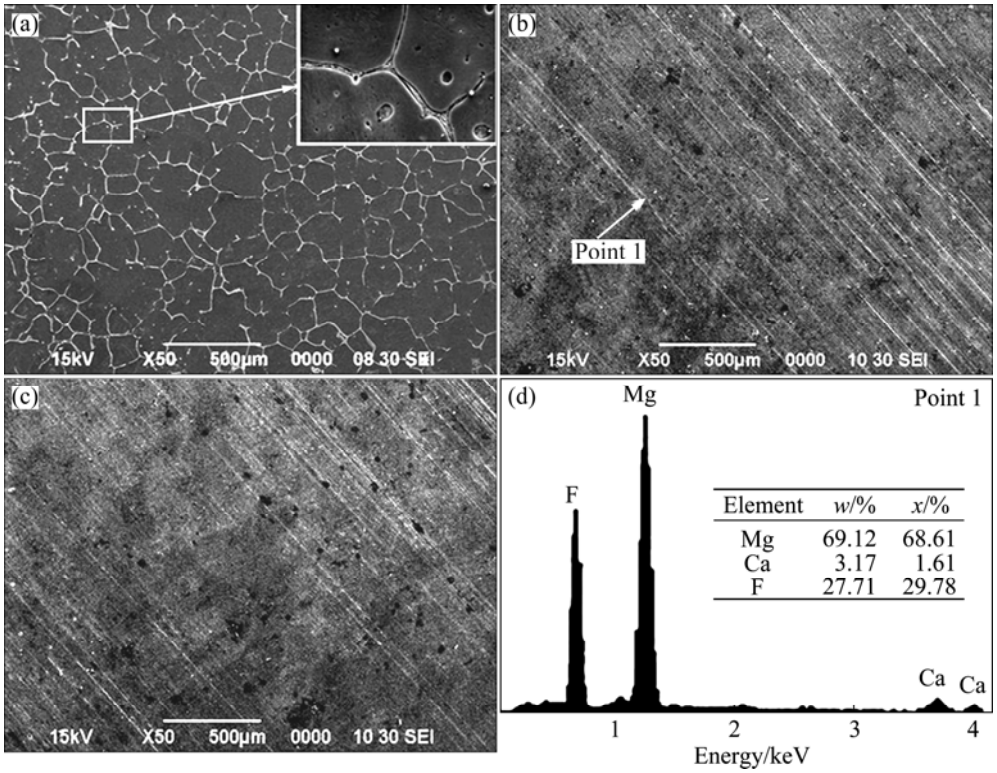

Fig. 4 SEM images of untreated (a), 35% HF (b), 40% HF (c) treated Mg−0.5Ca sample and EDS spectrum of point 1 (d)

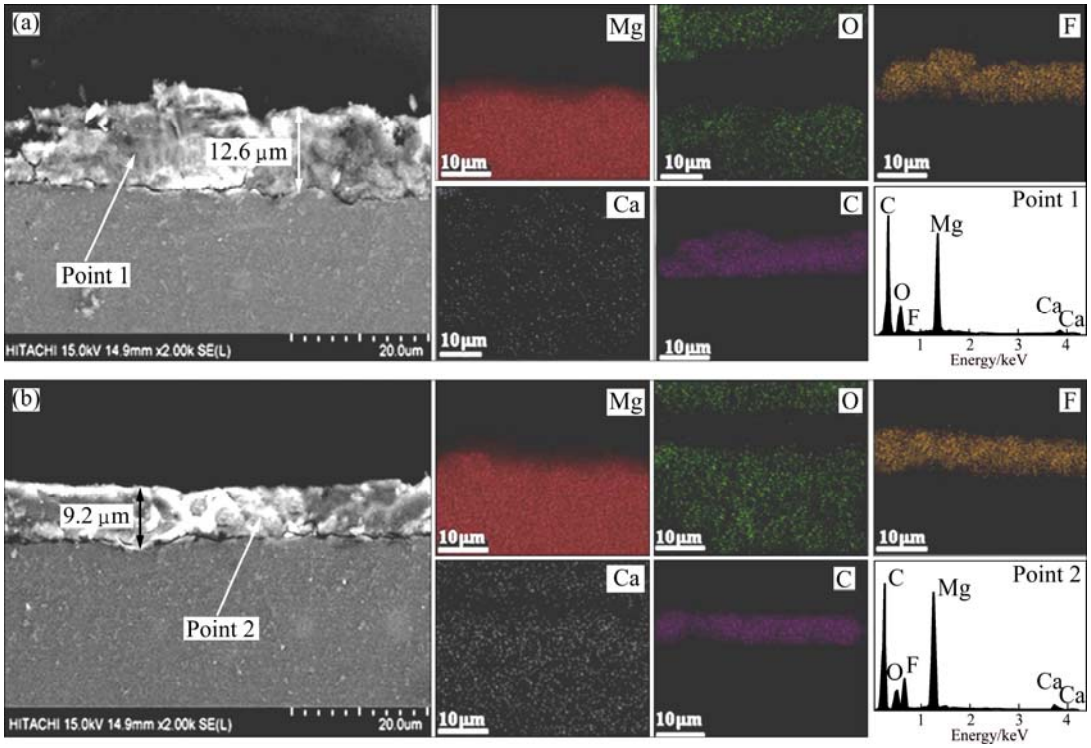

Fig. 5 SEM images and element mapping and corresponding EDS analysis of HF treated samples: (a) 40% HF; (b) 35% HF (Mg→red; Ca→blue; O→green; C→violent; F→yellow)

specimens revealed that the coating layers consist of Mg, Ca, O, C and F elements. The presence of fluoride showed that hydrofluoric acid was involved in the formation of the coating layer. The quantitative microprobe analyses of passive film showed a composition of 6.56% Mg, 0.43% Ca, 70.78% C, 13.84% O and 8.39% F (mole fraction) in 40% HF treated sample. The 35% HF treated sample composed of 6.24% Mg, 0.39% Ca, 72.31% C, 13.04% O and 8.02% F. The mole ratio of O to Mg was about 2.11 which indicated the formation of magnesium hydroxide $Mg(OH)_2$. These values were in good agreement with those found for the $Mg(OH)_2$ compound [26]. Element mapping of Mg, Ca, O, C and F elements of treated samples soaked in hydrofluoric for 24 h is depicted in Fig. 5. It can be seen that the calcium distributed homogeneously while carbon, magnesium and oxygen distributed heterogeneously. The yellow regions indicated that the fluoride distributed homogenously on the entire surface of specimens which showed the formation of compact protective film on the substrate. The red regions represent low content of Mg element. The high content of carbon in the coating layer can be attributed to hydrocarbons obtained from the environment (Figs. 5(c) and (d)). The presence of oxygen in protective film was due to hydrocarbons and hydroxides of $Mg(OH)_2$.

Figure 6 indicates the XRD patters of untreated and treated specimens. The XRD pattern of the untreated specimens showed high intensity of magnesium reflections with a preferred orientation along the (100), (112), (101), (102), (110) and (112) crystallographic planes respectively, accompanied by low intensities of Mg_2Ca phases with intensities of (313) reflection. However, XRD pattern of treated specimens indicated that the existence of tetragonal MgF_2 phases with intensities reflection of (110), (111) and (211) respectively, accompanied by matrix reflection.

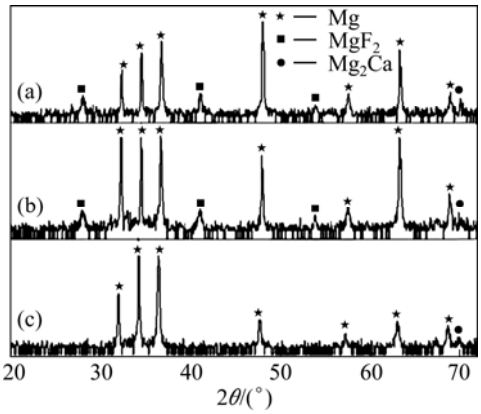

Fig. 6 XRD patterns of 40% HF (a), 35% HF (b) treated and (c) untreated specimens.

The averaged mean surface roughnesses (R_a) of treated and untreated samples are shown in Fig. 7. The surface roughness has strong influences on the corrosion

behaviors of the treated specimen. It was shown that the decline in surface roughness of sample led to a decrease in surface area for corrosive attack [27]. The results revealed that the untreated Mg−0.5Ca alloy specimens became coarser after fluoride treatments. The average roughness increased from 279 nm for untreated specimens to 370 nm and 305 nm for 35% HF and 40% HF treated specimens, respectively.

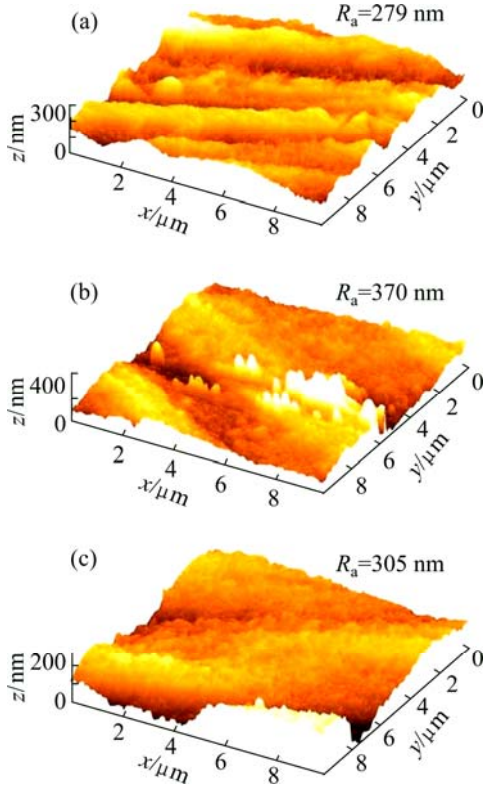

Fig. 7 AFM images of untreated (a), 35% HF (b), 40% HF (c) treated Mg−0.5Ca specimens

3.3 Electrochemical measurement

Figure 8 shows the electrochemical polarization curves of the untreated and treated specimens with 35% HF and 40% HF in Kokubo solution. The corrosion potential (φ_{corr}) of fluoride treated sample shifted to the nobler direction. For 40% HF treated specimen the φ_{corr} was 340 mV higher than did untreated specimens. In the case of 35% HF treated sample, the φ_{corr} shift was negligible compared with the 40% HF treated sample. However, corrosion current density (J_{corr}) decreases dramatically from 6.20 μA/cm^2 in 40% HF to 215 μA/cm^2 in naked specimens, which shows a high corrosion resistance of the treated sample compared with untreated specimens. KIM et al [28] proposed that formation of a micro-galvanic cell between the Mg_2Ca phase and Mg matrix led to enhanced dissolution rate of the Mg−0.5Ca untreated sample. However, in the case of fluoride treated specimen the presence of MgF_2 film, which acts as a protective layer on the surface of the sample, was the main reason of the corrosion rate reduction. It was reported that the protective layer blocked the reaction for transportation of species (such as water and chlorine) hence increasing the corrosion resistance of the sample [12,22]. The $\varphi_{pit}-\varphi_{OCP}$ represents the corrosion rate efficiency [15]. In this case a higher $\varphi_{pit}-\varphi_{OCP}$ value indicated a coating with more effective resistance. Table 2 shows that $\varphi_{pit}-\varphi_{OCP}$ values for 35% HF and 40% HF treated sample were 167 and 172 mV, respectively. In treated samples the cathodic current, which indicates the hydrogen evolution, declined with a lower slope compared with the one without coating as the applied potential increased. For bare sample the anodic current, which represents specimen dissolution, increased with a higher slope than the coated one as the applied potential increased. This phenomenon may be attributed to localized corrosion and subsequent pit propagation [10]. It is also observed that the φ_{corr} of specimens shifted to more negative potentials in the order of 40% HF<35% HF<untreated samples, which shows that the 40% HF treated sample has a high corrosion resistance compared with untreated Mg−0.5Ca alloy.

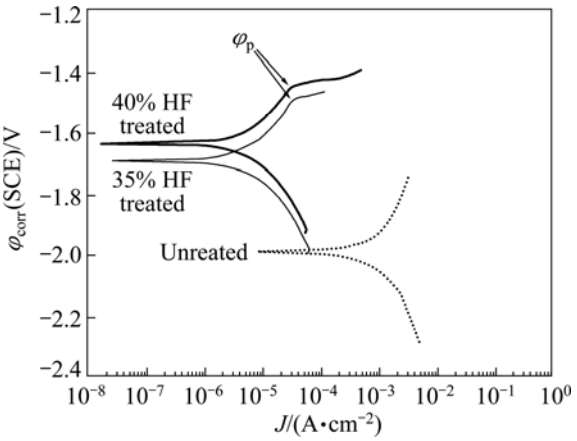

Fig. 8 Potentiodynamic polarization curves of untreated, 35% HF and 40% HF treated Mg−0.5Ca alloys in Kokubo solution

Table 2 Electrochemical parameters of untreated and fluoride coated specimens in Kokubo solution attained from polarization test

Specimen	φ_{corr}(SCE)/ mV	φ_{pit}(SCE)/ mV	J_{corr}/ (μA·cm^{-2})	Corrosion rate/(0.0254 mm·a^{-1})
Untreated Mg−0.5Ca	−1876	−	186	1520
35% HF treated sample	−1705	−1538	6.40	4.59
40% HF treated sample	−1658	−1486	6.20	2.89

Figure 9 shows the SEM images of the untreated and treated specimens after the polarization tests in Kokubo solution. Figure 9(a) shows the untreated sample

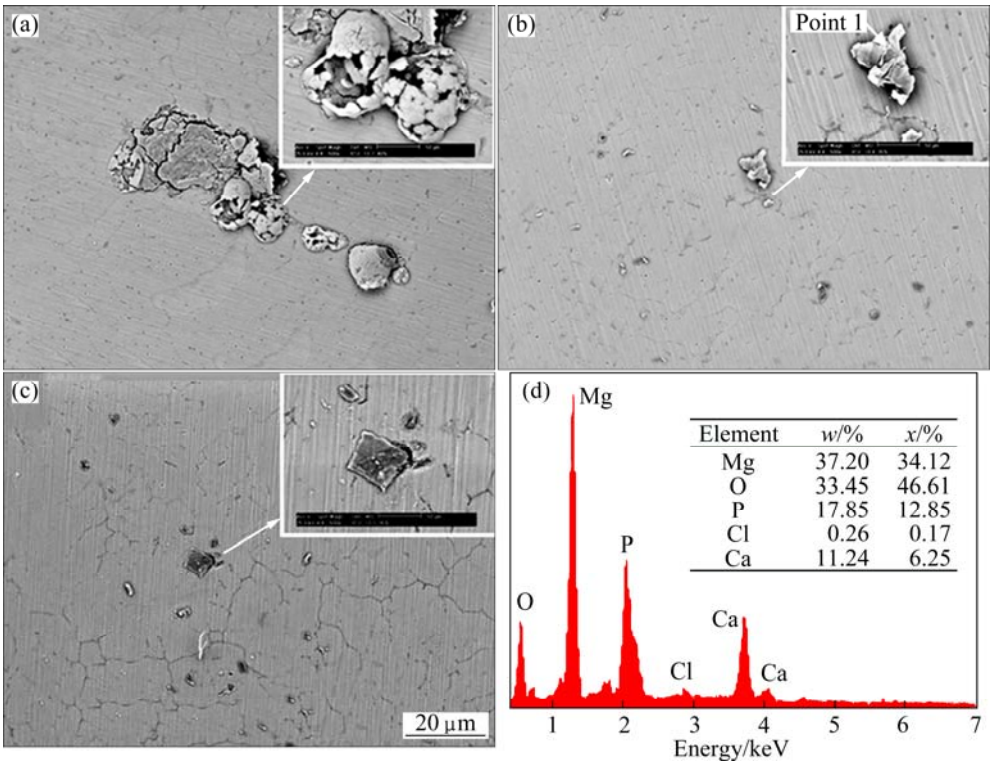

Fig. 9 SEM images and EDS spectrum analysis of specimens after potentiodynamic polarization tests: (a) Untreated; (b) 35% HF treated; (c) 40% HF treated; (d) EDS spectrum of point 1

suffering from plenty of round corrosion pits and some white particles. In low magnification several cracks distributed which some of them were covered with similar white particles. In high magnification the particles agglomerated next to deep crack of the corrosion layer. However, coated specimens showed uniform and smooth film containing only a small amount of white round particles (Figs. 9(b) and (c)). The EDS analysis of these particles indicated the presence of O, Mg, Ca, P and Cl elements in precipitation. In this case, 40% HF treated specimen showed more uniform film with lower round white particles compared with 35% HF treated specimen. The EDS analysis of white particles in 35% HF treated specimens showed a similar composition with 40% HF treated specimen.

3.4 In vitro degradation mechanism of fluoride coated Mg−0.5Ca alloy

Figure 10 exhibits the effect of fluoride coated Mg−0.5Ca samples on the mass loss of the alloy compared with the untreated Mg−0.5Ca sample in Kokubo solution for 7 d. According to the graph there was a significant increase in mass loss of untreated specimens in the first 72 h, after which the rate of loss decreases and remains constant afterwards. The main reason of fast degradation speed of untreated Mg−0.5Ca specimen in the earlier stage of immersion test was due

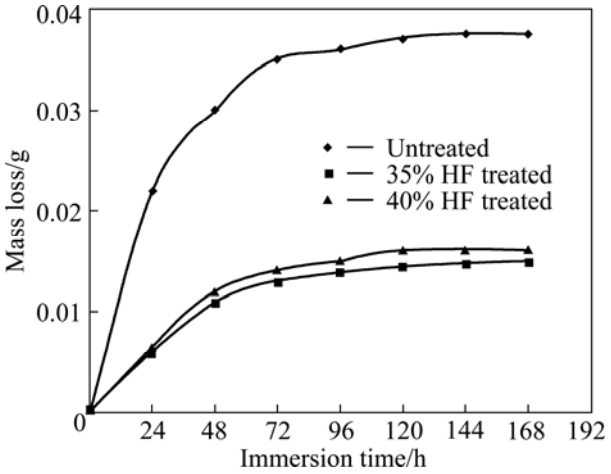

Fig. 10 Mass loss of untreated and treated specimens vs immersion time in Kokubo solution

to high chlorine concentration in SBF [29]. It was reported that high hydrogen evolution of untreated specimen led to an increase in the degradation rate. The aforementioned gas can accumulate around bare Mg−0.5Ca implant, resulting in serious side effects such as swelling in the vicinity of the treated part [30,31]. However, degradation rate decreases with increasing immersion time due to the deposition of hydroxyapatite (HA) on the untreated sample. The mass losses of treated specimens were noticeably lower than untreated

specimen for the entire stage (Fig. 10). This phenomenon was due to the formation of MgF_2 protective layer on the surface of the specimens which act as inhibitor to prevent from further corrosion. Furthermore, the fluoride coated layer decreased the blood content of alloying elements during the first 6 weeks of implantation [32]. Based on the mass loss after immersion for 7 d, the corrosion rate of untreated Mg−0.5Ca sample in Kokubo solution was 1.97 mm/a, whilst 35%HF and 40%HF treated samples degraded by 0.89 mm/a and 0.85 mm/a, respectively. LI et al [6] reported that the average degradation rate of Mg−0.5Ca alloy pins implanted in rabbit femora was about 2.28 mg/(mm^{-2}·a^{-1}). The rates of mass loss for both coated specimens increased with the immersion time in earlier stage, and subsequently mass loss decreased noticeably due to the escalated deposition of corrosion products and calcium phosphates on the samples [33]. The increase of calcium phosphate deposition resulted in accelerated mineral deposition rate on specimens when implanted into bone [15].

Two factors affect the degradation rate of fluoride Mg−0.5Ca alloy samples. The first is thickness of the coating layer. It was suggested that increasing the thickness of the dense layer prohibited further corrosion in Mg during tests in chloride solutions [15]. Surface roughness is another factor that influences the corrosion rate of treated samples. The 40% HF treated sample shows a lower degradation rate compared with 35% HF treated sample as a result of lower surface roughness of about 65 nm (Fig. 7) and thicker coating layer of around 3.4 μm

3.5 Immersion tests

Figure 11 shows SEM images of untreated and treated specimens after immersion in Kokubo solution for 168 h. Figure 11(a) shows corrosion product peeled off and a number of cracks with heterogeneous structures emerged in untreated specimens. The main reason of these cracks was due to water loss of the corrosion products and surface shrinkage. The EDS analysis shows the precipitates with high contents of Ca and P and low content of Mg. However, peeling area consisted of low contents of Ca and P and high content of Mg. High

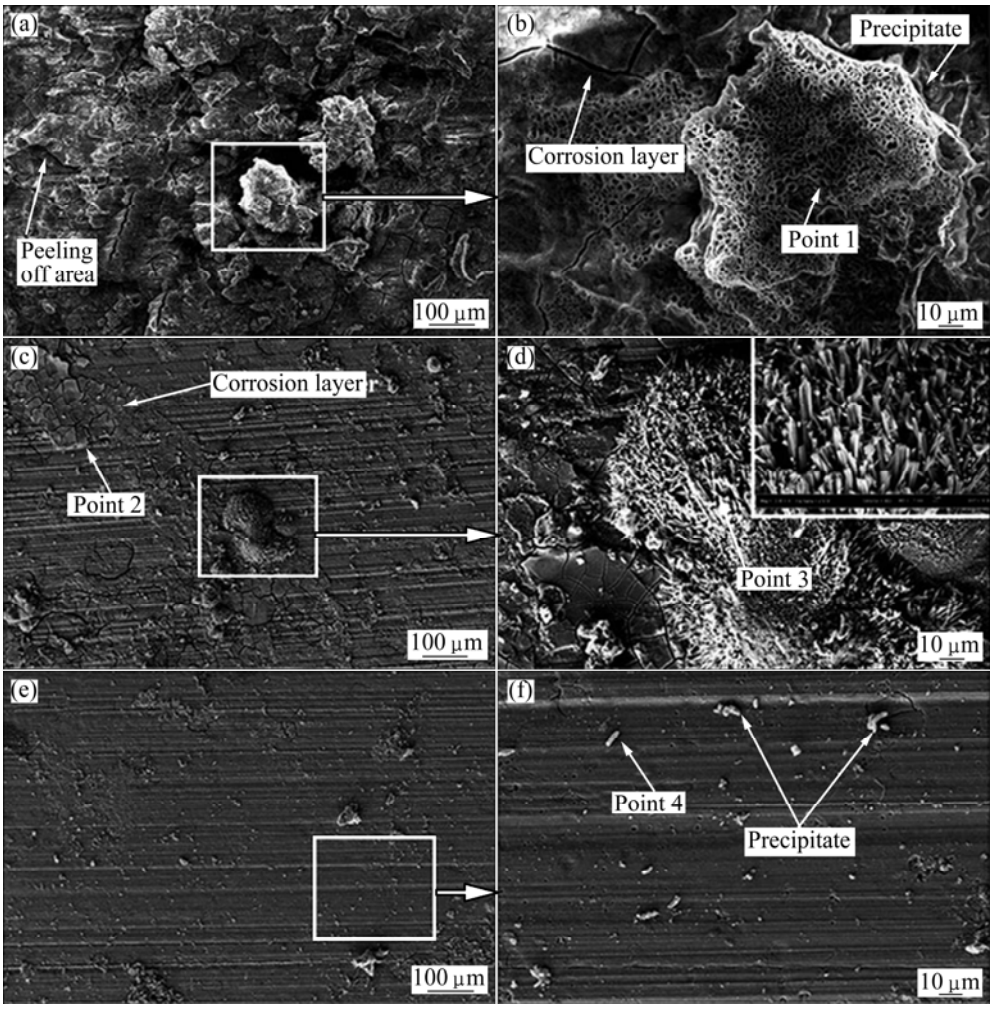

Fig. 11 SEM images of untreated (a,b), 35% HF (c,d) and 40% HF treated (e,f) Mg−0.5Ca alloy specimens with immersion duration of 168 h in SBF

magnification shows formation of porous deposit layer on some area of untreated sample. The thickness of this layer increased with increasing immersion time until it covers the entire surface of the sample. Magnesium dissolution and deposit layer formed according to the following reaction:

$$Mg \longrightarrow Mg^{2+}+2e \quad (4)$$

$$2H_2O+2e \longrightarrow H_2+2OH^- \quad (5)$$

$$Mg^{2+}+2OH^- \longrightarrow Mg(OH)_2 \quad (6)$$

$$Mg^{2+}+2Cl^- \longrightarrow MgCl_2 \quad (7)$$

The Cl^- in the solution transformed $Mg(OH)_2$ into soluble $MgCl_2$ [6,34,35], which then dissolved into Mg^{2+} and $2Cl^-$ causing an increase hydroxide (OH^-) ions near the surface of the sample. This leads to an increase in pH value of the solution. Subsequently phosphate (PO_4^{3-}) and Ca^{2+} in the solution reacted with OH^- to form $HA[Ca_{10}(PO_4)_6(OH)_2]$, which tended to nucleate and grow on the surface of untreated specimen. Figure 11(c) indicates surface morphology of the 35% HF treated specimens with closely packed needle-like crystals structure. This structure is similar to needle-like apatite nano-crystals in collagen matrix of human bone [18,36]. The treated specimens therefore have a high tendency to improve bone growth and hard tissue healing. The EDS results (Fig. 12) show that the needle-like structure contained high amount of Cl in the form of $MgCl_2$. However, with more dissolution of Mg, formation rate and driving force of $MgCl_2$ declined. Also EDS analyses indicated the presence of Ca, P, Mg, Na and F elements. The existence of Na^+, Mg^{2+} and F^- ions improved bioactivity in fluoride coated specimens due to similarity of composition with the natural bone minerals [18]. Moreover, needle-like morphology had more surface area exposed to the SBF solution causing more apatite formation on the surface to promote bone healing. Figure 11(e) displays precipitation of HA on the smooth surface of the 40% HF treated specimens. The EDS results identified the presence of Mg, O, Ca, P, Cl, C and F. Fluoride is a fundamental element in hard tissues and can improve the crystallization and mineralization of calcium phosphate for new bone formation [18,37]. The existence of C element in the protective layer was attributed to the dissolution of CO_2 in the air.

Figure 13 depicts the variation of pH values as a function of immersion time for untreated and fluoride treated samples. It has been reported that an increase in pH value resulted in potential haemolysis and it was not appropriate for growth and proliferation of cell [8,38,39]. The pH value of untreated specimen increased remarkably with increasing immersion time at the beginning stage of soaking as a result of dissolution of $Mg(OH)_2$ via Cl^- and OH^-. However, the pH value of

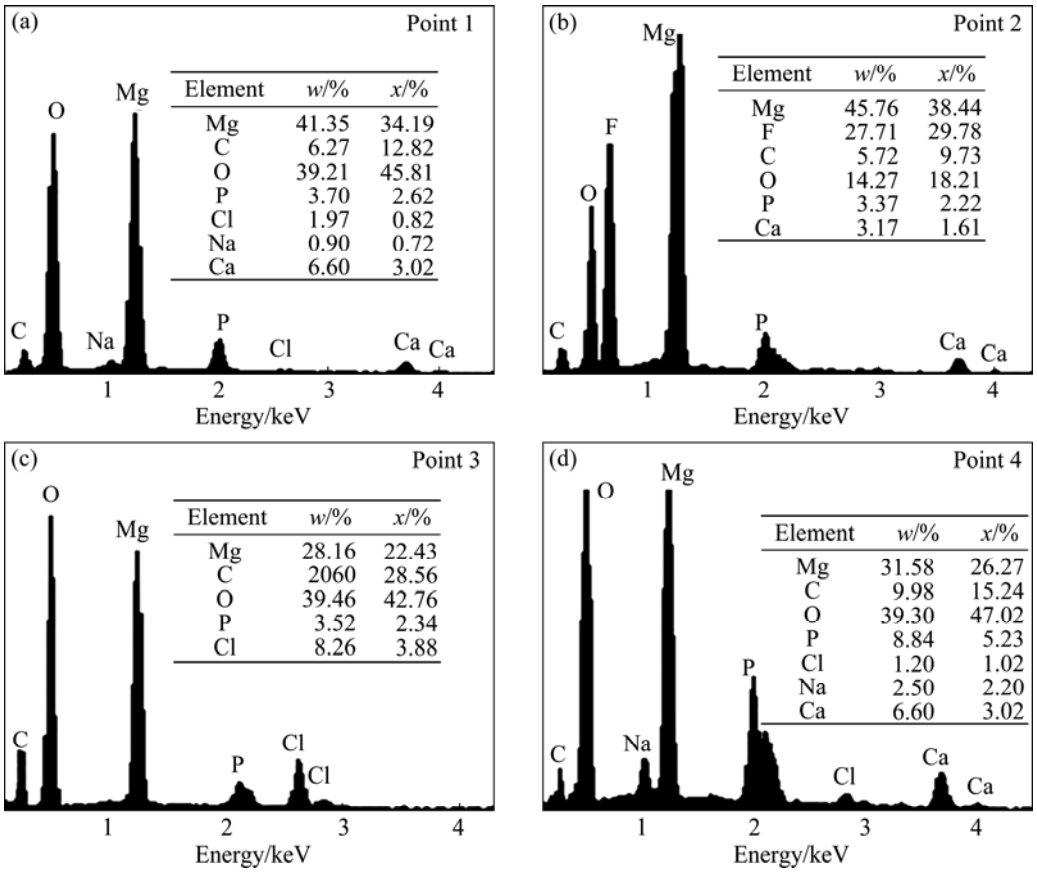

Fig. 12 EDS analyses of point 1 (a), point 2 (b), point 3 (c) and point 4 (d) in Fig. 11

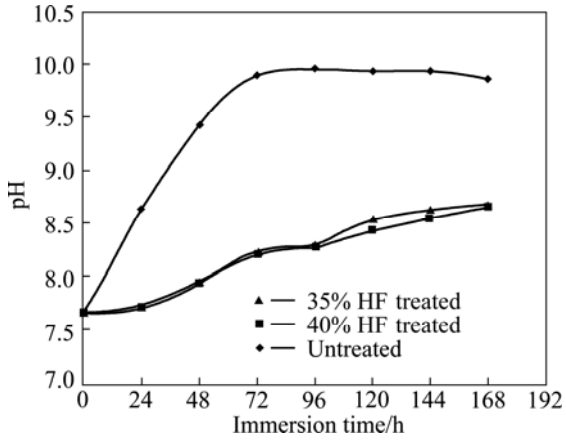

Fig. 13 Variation of pH value in SBF solution as function of immersion time for untreated and treated specimens

untreated specimens became constant after 72 h due to reaction between calcium and phosphate ions in the solution and provided a suitable condition for precipitation of HA. The pH values of the 35% HF and 40% HF treated samples were much lower than the untreated sample during the first 72 h. As a consequence, slower hydrogen evolution caused less OH^- compared with untreated specimen during the initial immersion time. However, precipitation of apatite which consumed OH^- ions could be the main reason of minimal pH increase at the final stage.

The facade of untreated and fluoride treated specimens after immersion tests in Kokubo solution at different time is shown in Fig. 14. After immersion some bubbles surrounded the untreated sample while there were no bubbles detected around treated samples. After 1 d of immersion, the naked sample contained several corrosion areas whilst no obvious corrosion products detected in the treated samples. After 3 d of immersion, untreated sample was covered with white corrosion products with small amount of corrosion products settled on the bottom of the beaker. However, the appearance of treated samples remained unchanged. This showed that the fluoride treatment significantly enhanced corrosion resistance of the samples. After 7 d of immersion, the 40% HF treated sample had better appearance compared with 35% HF treated sample, but the former showed corrosion dots on its surface. The appearance of treated samples changed slightly and became grayish. However, for the untreated sample the surface was fully covered with white corrosion products and showed delamination. These results revealed that the untreated sample suffered considerably from the environment while the fluoride treated sample showed significantly better performance for longer exposure time in corrosive solution.

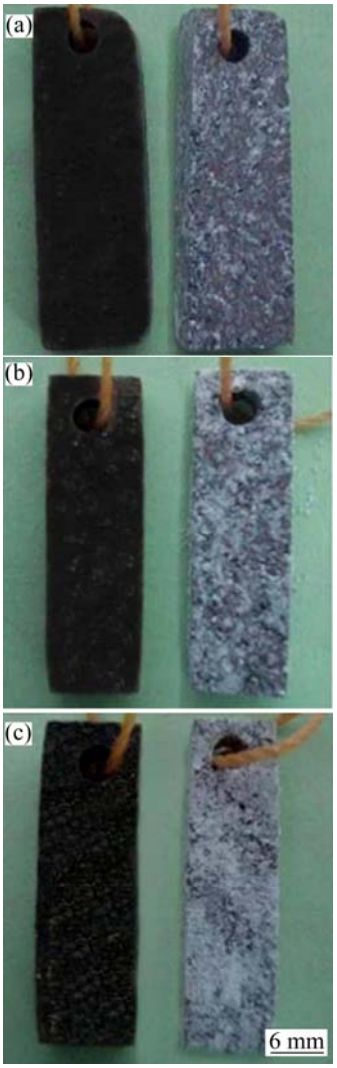

Fig. 14 Photos of untreated and fluoride treated Mg−0.5Ca alloys (Dark color: HF treated; Light color: untreated Mg−0.5Ca) after being immersed in Kokubo solution at 37 °C for 3 d (a), 7 d (b), 10 d (c)

4 Conclusions

1) Surface treatment of Mg−0.5Ca alloys by immersion in 40% HF provides a more uniform, denser and thicker coating layer (12.6 μm) compared with the 35% HF treated sample which results in a better protection of the substrate.

2) The electrochemical results reveal that the corrosion resistance of fluoride treated Mg−0.5Ca alloys is about 35 times higher compared with the untreated Mg−0.5Ca alloy specimen in Kokubo solution.

3) In vitro degradation rate of the fluoride treated specimens is significantly slower than that of untreated Mg−0.5Ca alloy in Kokubo solution. The fluoride treated specimens contained needle-like morphology, resulting in more apatite formation on the surface of sample to promote bone healing.

4) After immersion the 40% HF treated sample shows better appearance compared with 35% HF treated sample, but the former has several corrosion dots on its surface. However, the untreated specimen is fully covered by white corrosion products and show delamination.

5) Mg−0.5Ca alloy treated with 40% HF for 24 h is a promising candidate as biodegradable implants due to its low degradation kinetics and good biocompatibility.

Acknowledgment

This project was supported financially by Ministry of Higher Education of Malaysia under the Vote Number 78610. We would like to express our gratitude and deepest thanks to the Research Management Centre, Universiti Teknologi Malaysia (UTM), for managing the project.

References

[1] LOZANO R M, PEREZ-MACEDA B T, CARBONERAS M. Proteomic profile of osteoblastic cell cultured on fluoride-coated magnesium materials [C]//2nd Symposium on Biodegradable Metals. Maratea, Italy, 2010: 68.

[2] SUN Y, ZHANG B, WANG Y. Preparation and characterization of a new biomedical Mg−Zn−Ca alloy [J]. Materials and Design, 2012, 34: 58−64.

[3] CHIU K Y, WONG M H, CHENGA F T, MAN H C. Characterization and corrosion studies of fluoride conversion coating on degradable Mg implants [J]. Surface & Coating Technology, 2007, 202: 590−598.

[4] YU Bing-lung, LIN Jun-kai, UAN Jun-yen. Applications of carbonic acid solution for developing conversion coatings on Mg alloy [J]. Transactions of Nonferrous Metals Society of China, 2010, 20: 1331−1339.

[5] QIN Tie-nan, MA Li-qun, YAO Yan, NI Cong, ZHAO Xiang-yu, DING Yi. An in situ measure method to study deposition mechanism of electroless Ni−P plating on AZ31 magnesium alloy [J]. Transactions of Nonferrous Metals Society, 2011, 21: 2790−2797.

[6] LI Z, GU X, LOU S, ZHENG Y. The development of binary Mg–Ca alloys for use as biodegradable materials within bone [J]. Biomaterials, 2008, 29: 1329−44.

[7] OH-ISHIA K, WANTANABEB R, MENDISA C L. Age-hardening response of Mg–0.3 at.%Ca alloys with different Zn contents [J]. Materials Science and Engineering A, 2009, 526: 177–184.

[8] BAKHSHESHI-RAD H R, IDRIS M H, KADIR M R A, FARAHANY S. Microstructure analysis and corrosion behavior of biodegradable Mg–Ca implant alloys [J]. Materials and Design, 2012, 33: 88–97.

[9] SINGH S S, ROY A, LEE B, KUMTA P N. Deposition of calcium phosphate coatings on magnesium alloys by aqueous methods [C]//2nd Symposium on Biodegradable Metals. Maratea City, 2010: 95.

[10] WAN Y, XIONG G, LUO H. Preparation and characterization of a new biomedical magnesium–calcium alloy [J]. Materials and Design, 2008, 29: 2034−2037.

[11] JIANG Yong-feng, ZHOU Hai-tao, ZENG Su-min. Microstructure and properties of oxalate conversion coating on AZ91D magnesium alloy [J]. Transactions of Nonferrous Metals Society, 2009, 19: 1416−1422.

[12] ZHOU W, SHAN D, HAN E H, KE W. Structure and formation mechanism of phosphate conversion coating on die-cast AZ91D magnesium alloy [J]. Corrosion Science, 2008, 50: 329−337.

[13] HEAKAL F E T, FEKRY A M, FATAYERJI M Z. Influence of halides on the dissolution and passivation behavior of AZ91D magnesium alloy in aqueous solutions [J]. Electrochimica Acta, 2009, 54: 1545−1557.

[14] ZHANG T, SHAO Y, MENGA G. Effects of hydrogen on the corrosion of pure magnesium [J]. Electrochimica Acta, 2006, 52: 1323−1328.

[15] GU X N, ZHENG W, CHENG Y, ZHENG Y F. A study on alkaline heat treated Mg−Ca alloy for the control of the biocorrosion rate [J]. Acta Biomaterialia, 2009, 5: 2790−2799.

[16] LI W, ZHUA L, LIA Y, ZHAO B. Growth characterization of anodic film on AZ91D magnesiumalloy in an electrolyte of Na_2SiO_3 and KF [J]. University of Science and Technology Beijing: Mineral, Metallurgy, Material, 2006, 13: 450−455.

[17] CONCEICAO T F D, SCHARNAGL N, BlLAWERT C, et al. Surface modification of magnesium alloy AZ31 by hydrofluoric acid treatment and its effect on the corrosion behaviour [J]. Thin Solid Films, 2010, 518: 5209−5218.

[18] MENG E C, GUAN S K, WANG H X, WANG L G, ZHU S J, HU J H, REN C X, GAO J H, FENG Y S. Effect of electrodeposition modes on surface characteristics and corrosion properties of fluorine-doped hydroxyapatite coatings on Mg−Zn−Ca alloy [J]. Applied Surface Science, 2011, 257: 4811−4816.

[19] CHIU L H, CHEN C C, YANG C F. Improvement of corrosion properties in an aluminum-sprayed AZ31 magnesium alloy by a post-hot pressing and anodizing treatmen [J]. Surface & Coating Technology, 2005, 191: 181−187.

[20] THOMANN M, KRAUSE C, ANGRISANI N, BORMANN D, HASSEL T, WINDHAGEN H, MEYER L A. Influence of a magnesium-fluoride coating of magnesium-based implants (MgCa0.8) on degradation in a rabbit model [J]. Journal of Biomedical Materials Research, 2010, 93: 1609−1619.

[21] CHEN Jun, SONG Ying-wei, SHAN Da-yong, et al. Properties of dawsonite conversion film on AZ31 magnesium alloy [J]. Transactions of Nonferrous Metals Society, 2011, 21: 936−942.

[22] GU X N, LI N, ZHOU W R, et al. Corrosion resistance and surface biocompatibility of a microarc oxidation coating on a Mg−Ca alloy [J]. Acta Biomaterialia, 2011, 7: 1880−1889.

[23] ELSENTRIECY H H, AZUMI K, KONNO H. Effect of surface pretreatment by acid pickling on the density of stannate conversion coatings formed on AZ91 D magnesium alloy [J]. Surface & Coating Technology, 2007, 202: 532−537.

[24] DRYNDA A, HASSEL T, HOEHN R, PERZ A, BACH F W, PEUSTER M. Development and biocompatibility of a novel corrodible fluoride-coated magnesium- calcium alloy with improved degradation kinetics and adequate mechanical properties for ardiovascular applications [J]. Journal of Biomedical Materials Research, 2009, 93: 763−775.

[25] ASTM G31-72. Standard practice for laboratory immersion corrosion testing of metals [R]. 2004.

[26] VERDIERC S, LAAKA N V D, DELALANDEA S. The surface reactivity of a magnesium–aluminium alloy in acidic fluoride solutions studied by electrochemical techniques and XPS [J]. Applied Surface Science, 2004, 253: 513−524.

[27] BUDKE E, KREMPEL H J, MAIDHOF H, SCHUSSLER H. Decorative hard coatings with improved corrosion resistance [J]. Surface & Coating Technology, 1999, 112: 108−113.

[28] KIM W C, KIM J G, LEE J Y. Influence of Ca on the corrosion properties of magnesium for biomaterials [J]. Materials Letters, 2008, 62: 4146−4148.

[29] WEN C, PENG L, REN C, WANG X, HU Z. Characterization and

degradation behavior of AZ31 alloy surface modified by bone-like hydroxyapatite for implant applications [J]. Applied Surface Science, 2009, 225: 6433−6438.

[30] WENG H, ESTRIN Y, ZUBEROVA Z. Bio-corrosion of a magnesium alloy with different processing histories [J]. Materials Letters, 2008, 62: 2476−2479.

[31] KOLEINI S, IDRIS M H, JAFARI H. Influence of hot rolling parameters on microstructure and biodegradability of Mg−1Ca alloy in simulated body fluid [J]. Materials and Design, 2012, 33: 20−25.

[32] WITTE F, FISCHER J, NELLESEN J. In vivo corrosion and corrosion protection of magnesium alloy LAE442 [J]. Acta Biomaterialia, 2010, 6: 1792−1799.

[33] WANGA H, GUANA S, WANG Y. In vivo degradation behavior of Ca-deficient hydroxyapatite coated Mg−Zn−Ca alloy for bone implant application [J]. Colloids Surf B Biointerfaces 2011, 88: 254−259.

[34] ZHANG S, ZHANG X, ZHAO C. Research on an Mg−Zn alloy as a degradable biomaterial [J]. Acta Biomaterialia, 2010, 6: 626−640.

[35] ZHANG S, LI J, SONG Y. In vitro degradation, hemolysis and MC3T3-E1 cell adhesion of biodegradable Mg−Zn alloy [J]. Materials Science and Engineering C, 2009, 29: 1907−1912.

[36] LI Jian-zhong, HUANG Jiu-gui, TIAN Yan-wen. Corrosion action and passivation mechanism of magnesium alloy in fluoride solution [J]. Transactions of Nonferrous Metals Society of China, 2009, 19: 50−54.

[37] WANG Y, ZHANG S, ZENG X. Osteoblastic cell response on fluoridated hydroxyapatite coatings [J]. Acta Biomaterialia, 2007, 3: 191−197.

[38] ZHANG E, YANG L, XU J, CHEN H. Microstructure, mechanical properties and biocorrosion properties of Mg−Si(−Ca, Zn) alloy for biomedical application [J]. Acta Biomaterialia, 2010, 6: 1756−1762.

[39] ZHANG E, YIN D, XU L, YANG L, YANG K. Microstructure, mechanical and corrosion properties and biocompatibility of Mg−Zn−Mn alloys for biomedical application [J]. Materials Science and Engineering C, 2009, 29: 987−993.

氟化处理对植入材料 Mg−Ca 二元合金腐蚀行为的影响

Hamid Reza Bakhsheshi-Rad[1], Mohd Hasbullah Idris[1],
Mohammed Rafiq Abdul Kadir[2], Mohammadreza Daroonparvar[1]

1. Materials Engineering Department, Faculty of Mechanical Engineering,
Universiti Teknologi Malaysia, Skudai 81310, Johor, Malaysia;
2. Department of Biomechanics & Biomedical Materials, Faculty of Biomedical Engineering & Health Sciences,
Universiti Teknologi Malaysia, Skudai 81310, Johor, Malaysia

摘　要：在室温下，将 Mg−0.5Ca 合金在不同浓度的氢氧化钠和 HF 溶液浸渍不同的时间,研究 HF 处理对合金腐蚀行为的影响。采用原子力显微镜、X 射线衍射、场发射扫描电子显微镜表征样品的微观组织变化。通过动电位极化和 Kokubo 溶液浸泡试验测试样品的耐腐蚀性。结果表明，与 35% HF 处理的样品相比，经 40% HF 溶液处理的 Mg−0.5Ca 合金具有更均匀、更致密、更薄的涂层(12.6 μm)。电化学测试表明，在 Kokubo 溶液中，经氟化物处理的 Mg−0.5Ca 合金样品的耐腐蚀性比未处理样品的高 35 倍；前者的体外降解速率远远低于后者的。在 40% HF 溶液处理过的样品表面只出现了一些腐蚀点，而未经处理的样品完全被腐蚀产物覆盖且出现了分层现象。40% HF 处理的 Mg−0.5Ca 合金，具有低的降解速率和良好的生物相容性，是一种有潜力的植入材料。

关键词：Mg−Ca 合金；表面处理；腐蚀行为；生物相容性

(Edited by Xiang-qun LI)